

Optical Measurement of the Deformation of Giant Lipid Vesicles Driven by a Micropipet Electrode

Chau-Hwang Lee,* Yu-Fen Chang, Chia-Hsuan Tsai, and Po-Hsiang Wang

Research Center for Applied Sciences, Academia Sinica, 128 Sec. 2, Academia Rd.,
Nankang, Taipei 11529, Taiwan

Received May 11, 2005

We investigate the deformation of giant lipid vesicles driven by a micropipet electrode by use of differential confocal microscopy. This optical technique provides nanometer depth resolution without mechanical contact and hence prevents large tension or perforation of the soft membrane. For dipalmitoyl phosphatidylcholine (DPPC) membranes in the gel phase, we observed deformations of several hundreds of nanometers when the driving voltage was about 0.1 V. The voltage and frequency responses of the vesicle deformation can be explained by the balance between the electroosmotic force inside the micropipet and the membrane tension. We also used DPPC:cholesterol vesicles to check the validity of this model. In the fluid phase, however, the deformation is independent of the modulation signal because micrometer-scale thermal fluctuations dominate the membrane motion.

Introduction

The deformation of giant lipid vesicles (GLVs) induced by external electric field provides a mechanism to control the curvature and tension of the membrane at high frequencies, and therefore it has been studied theoretically^{1,2} and experimentally.³ Most of the previous works were focused on the large deformation induced by a pair of parallel electrodes beside the vesicle. Asymmetric charge accumulation on the internal or external surface of the membrane by ion adsorption can also cause evident shape changes of GLVs.⁴ In these experimental studies, the vesicles were left untouched and the deformation was observed through optical microscopy. Owing to the limit of optical resolution, the vesicles must be deformed for several micrometers to be quantitatively characterized. In addition to parallel electrodes and ion adsorption, the microelectrode technique based on a micropipet may also be used to apply voltage on a GLV. With a micropipet, the membrane area and tension can be changed and the mechanical properties such as bending rigidity can be deduced.^{5,6} Nevertheless, using the voltage through a micropipet electrode to change the shape of GLVs has not been demonstrated yet. A possible reason could be the small deformation caused by the limited electrode voltage when electroporation is not allowed. For parallel electrodes, electric fields as large as several kV/cm are required to induce observable deformations of GLVs with a phase-contrast optical microscope.³ Such large electric fields will induce electroporation of the membrane if they are applied by a microelectrode. With smaller electrical fields, the deformation could be in the submicrometer regime, and therefore techniques with resolution much better than conventional optical microscopy should be employed to

explore the relation between the deformation of GLVs and the voltage applied by a microelectrode.

In this work, we use differential confocal microscopy (DCM),^{7,8} a far-field optical technique with nanometer depth resolution, to characterize the electrically driven deformation of GLVs. DCM has been successfully applied to measuring the bending rigidity of GLV membranes in various phases.⁹ The advantageous features of DCM include the negligible optical force exerted by probing light on the membrane and the ability of real-time recording of the membrane position. In the DCM study of bending rigidity, a vesicle was preserved after more than 12 h of observation at various temperatures. Micromanipulation with micropipets is also easy to incorporate with DCM because DCM employs a conventional objective lens as the probe, of which the working distance is hundreds of micrometers. With these features, DCM is very suitable for measuring the electrically driven deformation of GLVs.

Materials and Methods

Vesicle Preparation. The vesicles were prepared by the organic evaporation method.¹⁰ Lipid dipalmitoyl phosphatidylcholine (DPPC) purchased from Sigma-Aldrich, St. Louis, MO, was dissolved in chloroform:methanol (volume ratio 2:1), spread on the glass substrate of a culture dish, and then placed in a vacuum overnight to form a lipid film. The dried DPPC film was prehydrated by water-saturated nitrogen gas, and then a buffer solution consisting of 0.1-M KCl and 0.1-M sucrose was gently added. The sample was incubated at 50 °C for longer than 12 h, and then a “cloudy” fraction appeared on the bottom of the culture dish. GLVs (10–40 μm in diameter) selected for the measurement were harvested from the cloudy fraction and were placed into a clean polyethylene Petri dish containing 0.1-M KCl and 0.1-M dextrose aqueous solution. A copper coil under the Petri dish was used to set the temperature higher than the room temperature when it was necessary. The unilamellarity of the vesicle membranes was verified by phase-contrast optical microscopy.¹¹

Voltage Application. Thin-walled borosilicate glass micropipets filled with the same solution as that in the Petri dish was used to apply voltage on the vesicle. The micropipet was

* To whom correspondence should be addressed. Phone: 886-2-27898000 ex 18; fax: 886-2-27826680; e-mail: clee@gate.sinica.edu.tw.

(1) Kummrow, M.; Helfrich, W. *Phys. Rev. A* **1991**, *44*, 8356–8360.
(2) Hyuga, H.; Kinoshita, K., Jr.; Wakabayashi, N. *Bioelectrochem. Bioenerg.* **1993**, *32*, 15–25.

(3) Riske, K. A.; Dimova, R. *Biophys. J.* **2005**, *88*, 1143–1155.
(4) Petrov, P. G.; Lee, J. B.; Dobereiner, H.-G. *Europhys. Lett.* **1999**, *48*, 435–441.

(5) Evans, E.; Rawicz, W. *Phys. Rev. Lett.* **1990**, *64*, 2094–2097.
(6) Zhelev, D. V.; Needham, D.; Hochmuth, R. M. *Biophys. J.* **1994**, *67*, 720–727.

(7) Lee, C.-H.; Wang, J. *Opt. Commun.* **1997**, *135*, 233–237.

(8) Lee, C.-H.; Guo, C.-L.; Wang, J. *Opt. Lett.* **1998**, *23*, 307–309.

(9) Lee, C.-H.; Lin, W.-C.; Wang, J. *Phys. Rev. E* **2001**, *64*, 020901.

(10) Akashi, K.; Miyata, H.; Itoh, H.; Kinoshita, K., Jr. *Biophys. J.* **1996**, *71*, 3242–3250.

(11) Servuss, R. M.; Boroske, E. *Phys. Lett. A* **1979**, *69*, 468–470.

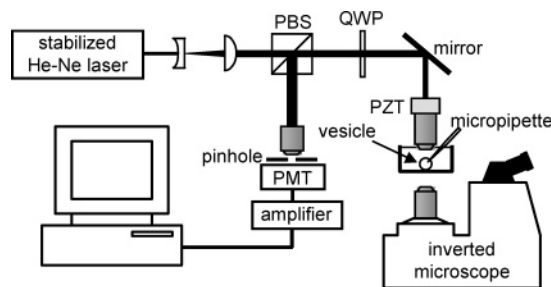


Figure 1. Scheme of the experimental setup. PBS, polarization beam splitter; PMT, photomultiplier tube; PZT, piezoelectric transducer; QWP, quarter wave plate.

inserted in an electrode holder containing a pressure port and a Ag/AgCl electrode (Warner Instruments, Hamden, CT). The other electrode was placed inside the bath solution as the reference. With a typical tip aperture of $2\ \mu\text{m}$, the micropipet had a resistance of $2\text{--}5\ \text{M}\Omega$ when placed in the solution. The micropipet contacted the vesicle in the cell-attached configuration, and the membrane remained intact during the measurement. If the membrane was broken, the vesicle shrank owing to the suction of the pipet, and we discarded that vesicle. A vesicle was aspirated by the micropipet to a seal resistance close to or above $100\ \text{M}\Omega$, slightly lifted from the dish bottom, and placed within the measurement dynamic range of DCM. Because slight fluctuations severely affected the accuracy of measurement, we started the experiments after the system was left untouched for at least 30 min. A function generator was used to apply voltage on the vesicle, and a low-noise current-to-voltage amplifier (Stanford Research Systems, Stanford, CA, model SR-570) was used to detect the transmembrane current signal for the determination of the seal resistance.

DCM. Figure 1 shows the scheme of the experimental setup, which was placed on an optical bench equipped with an active vibration isolation system. In brief, a stabilized 633-nm He-Ne laser (Melles Griot, Carlsbad, CA, model 05-STP-901) with power fluctuation less than 0.2% was used as the light source for measuring the membrane deformation. The laser beam was focused on the vesicle with a $40\times$, $0.75\ \text{numerical aperture}$ water-immersion objective lens. The optical power after the objective lens was $0.7\ \text{mW}$, and the reflectivity of DPPC membranes in water was $\sim 0.02\%$.⁹ Light reflected from the membrane was detected with a photomultiplier tube (PMT) behind a $5\text{-}\mu\text{m}$ pinhole. The output signal of the PMT was filtered by a low-pass filter of which the cutoff frequency was set to 30 Hz, digitized by a 16-bit analogue-to-digital converter, and then was stored in a personal computer for further analyses. The setup resembled a confocal microscope, while we used a piezoelectric transducer (PZT) to precisely control the height of the focal plane relative to the membrane surface. As the membrane surface was about $0.5\ \mu\text{m}$ away from the focal plane, the reflected signal detected by the PMT was very sensitive to the height variation. Therefore, this setup can easily detect nanometer deformation of the membranes. More details of the calibration and operation of DCM can be found in our previous articles.^{7–9} In addition to the high sensitivity and small mechanical pressure, another advantage of using DCM in this study was that the electrical driving signal was intrinsically isolated from the optical signal of membrane motion.

Figure 2 shows the stability of the micropipet during measurement. We sucked a DPPC vesicle with the micropipet and applied a $0.1\ \text{V}$ sinusoidal signal on the electrode. Then, we focused the laser spot on the micropipet tip to see if the position of the glass micropipet responded to the applied voltage. The result in Figure 2 shows no evidence of such effects. The fluctuations of the micropipet were within $\pm 12.4\ \text{nm}$ (one standard deviation for 3000 data points) and did not show any significant features related to the driving voltage.

Results and Discussion

Voltage-Induced Vesicle Deformation in the Gel Phase. As a first step, we kept the whole system at $23\ ^\circ\text{C}$ so that the DPPC membrane was in the gel phase. Figure

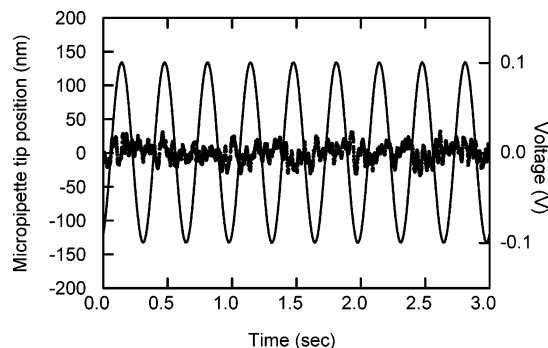


Figure 2. Position of the micropipet tip driven by a $0.1\ \text{V}$ sinusoidal signal when the tip sucked a DPPC vesicle with $100\ \text{M}\Omega$ seal resistance. Dots, tip position detected by DCM. Line, applied voltage. The tip fluctuation is independent of the applied voltage.

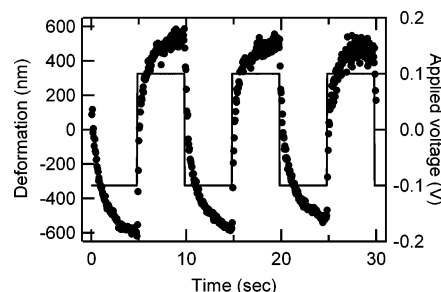


Figure 3. Vesicle deformation caused by $0.1\ \text{V}$ driving voltage. Dots, membrane position detected by DCM. Line, applied voltage. The modulation frequency is $0.1\ \text{Hz}$. During the measurement, the temperature was kept at $23\ ^\circ\text{C}$.

3 shows the vesicle deformation in response to the applied voltage of a square waveform. The diameter of the vesicle was $\sim 35\ \mu\text{m}$. With the submicrometer deformation, the vesicle survived more than 1000 cycles of undulation. In Figure 3, we also found that the deformation saturated at $\sim 600\ \text{nm}$, about 1.8% the diameter of the vesicle. Such small deformation was difficult to quantify by using conventional optical images.

With modulation of sinusoidal waveforms, we could easily characterize the voltage and frequency responses of the GLV deformation. Figure 4 shows the membrane response of a DPPC vesicle under the modulation of $0.1\ \text{V}$, $3\ \text{Hz}$ driving voltage. The diameter of this vesicle was $\sim 40\ \mu\text{m}$. The phase delay between the applied voltage and the membrane deformation is about 1.4π radians. We noted that the phase delay could be as large as 2π radians in some cases. This phase delay implies that the deformation of the vesicle may not be driven directly by the voltage signal. We will discuss the driving mechanism in the following section. The spectrum of the membrane motion is shown in Figure 4b and the amplitude of the deformation at $3\ \text{Hz}$ is $600\ \text{nm}$.

By changing the amplitude of the driving voltage, we characterized the voltage response of a DPPC vesicle. Figure 5 shows the linear voltage response of the vesicle deformation. Meanwhile, Figure 6 shows the frequency response of the deformation. Both results were obtained on the same specimen. A linear fitting of the logarithmic values shows that the deformation is inversely proportional to the square root of the driving frequency.

Mechanism of the Vesicle Deformation. Here, we propose a mechanism of the vesicle deformation on the basis of the characteristics in Figures 3–6. In cell-attached configuration with the seal resistance around $100\ \text{M}\Omega$, most of the voltage drop is across the tip, and thus strong

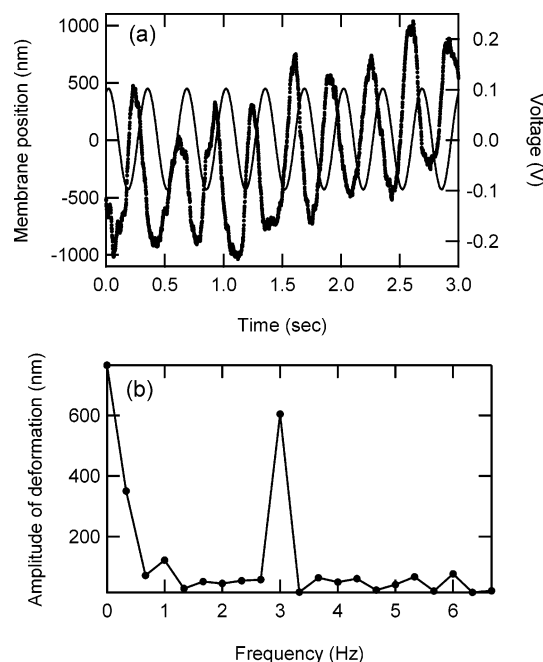


Figure 4. (a) Membrane movement of a 40- μm DPPC vesicle in the gel phase caused by 0.1 V driving voltage. Dots, membrane position. Solid line, applied voltage. The modulation frequency is 3 Hz. (b) Spectrum of the membrane movements in a. During the measurement, the temperature was kept at 23 $^{\circ}\text{C}$.

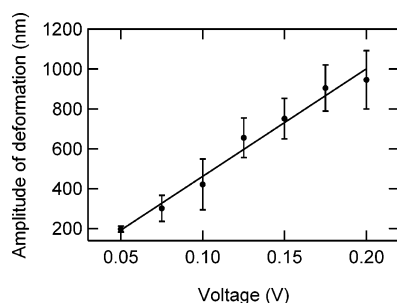


Figure 5. Deformation of a DPPC vesicle driven at 3 Hz. The diameter of this vesicle is 39 μm , and the effective sealing resistance of the patch is 97 M Ω . Dots, amplitudes of deformation. The error bars represent the standard deviation of five measurements. All the data were obtained on the same specimen. Solid line, a linear fitting shows the deformation is proportional to the driving voltage. During the measurement, the temperature was kept at 23 $^{\circ}\text{C}$.

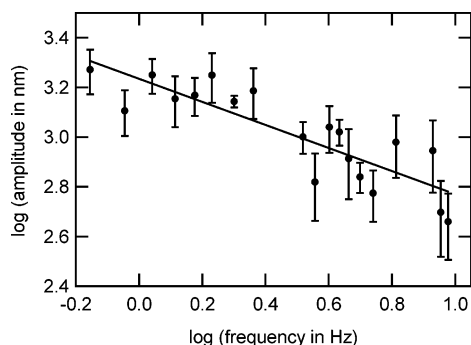


Figure 6. Frequency response of the DPPC vesicle deformation driven at 0.1 V. The error bars represent the standard deviation of five measurements on the same vesicle. Solid line, a fitting line of which the slope is -0.46 ± 0.07 . During the measurement, the temperature was kept at 23 $^{\circ}\text{C}$.

electroosmosis near the tip can be expected. Recently, electroosmotic flow has been used to explain the electrically driven motion of DNA molecules near the tip of a

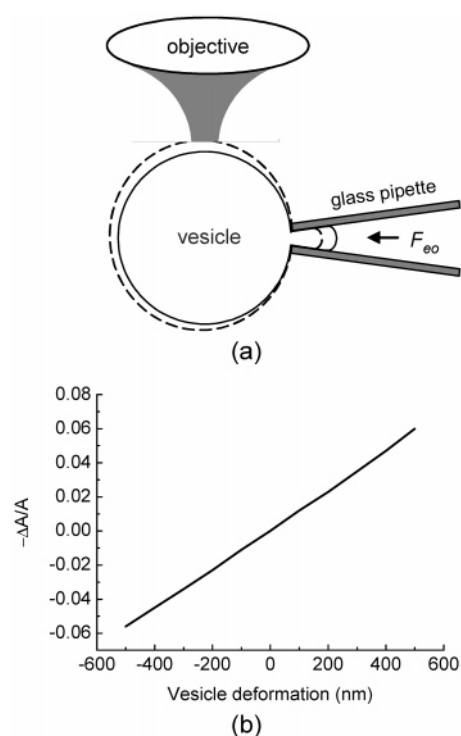


Figure 7. (a) Scheme of the measurement in this study when positive voltage is applied. (b) The relative change of surface area versus the measured deformation on top of the vesicle.

nanopipet.¹² Here, we also use the electroosmotic force to depict the observations in our experiments. The wall of a glass micropipet is negatively charged in electrolyte, and therefore a diffuse layer of positive charges appears beside the wall surface.¹³ As the electrode inside the micropipet is positively biased, an outward electroosmotic force is produced by the flow of the diffuse layer. The sucked vesicle is thus pushed out by this electroosmotic flow. As the vesicle is deformed, the electroosmotic force should be balanced such that the deformation saturates, as shown in Figure 3. In our experiments, the only force that can resist the outward electroosmotic force is the surface tension when the surface area of the vesicle is reduced. On the basis of the above description, in the following paragraphs we deduce a linear relation between the driving voltage and the vesicle deformation.

The relation between surface tension τ and relative area change is

$$\tau = K_s \cdot \Delta A / A_0 \quad (1)$$

where ΔA is the change of surface area, A_0 is the original surface area, and K_s is the area compressibility of the membrane.¹⁴ Because the electroosmotic force F_{eo} is proportional to the applied voltage V in a cylindrical pipet¹³ and the tension force $F_t = 2\pi a\tau$ (a is the inner radius of the micropipet), as the change of a is assumed to be negligible during the electrical modulation, the force-balance condition ($F_{eo} = F_t$) leads to $\tau \propto V$.

In this study, we measured the deformation of a vesicle on top of it, as shown in Figure 7a. Assuming the volume of vesicle is constant during the deformation,⁵ the relation between the measured deformation Δr and the change of

(12) Ying, L.; White, S. S.; Bruckbauer, A.; Meadows, L.; Korchev, Y. E.; Klennerman, D. *Biophys. J.* **2004**, *86*, 1018–1027.

(13) Adamson, A. W. *Physical Chemistry of Surfaces*, 5th ed.; Wiley: New York, 1990; Chapter 5.

(14) Evans, E.; Kwok, R. *Biochemistry* **1982**, *21*, 4874–4879.

surface area can be calculated by simple geometry, and the result is shown in Figure 7b. The measured deformation is in proportion to the negative relative change of surface area. This is consistent to the experimental results: when we applied positive voltage, a raise of the membrane position was detected, which corresponded to a decrease of the surface area. Therefore, the tension was toward the interior of the micropipet and against the electroosmotic force. Since the measured deformation is in proportional to $\Delta A/A_0$, it is also proportional to τ because of eq 1. Hence, at the force balance $\Delta r \propto \tau \propto V$. The above explanation is consistent to the experimental result shown in Figure 5.

The $1/\sqrt{f}$ frequency response in Figure 6 can be understood from energy conservation. Because the membrane surface area changed during the electrically driven deformation (Figure 7b), the membrane stretching elastic energy varied accordingly. For a lipid membrane, the change of stretching elastic energy per unit area is¹⁵

$$\Delta w_s = \frac{K_s}{2} \left(\frac{\Delta A}{A_0} \right)^2 \quad (2)$$

From eq 2, we can deduce the change of stretching elastic energy with the change of vesicle radius Δr as the independent variable (neglecting the highest-order term of Δr):

$$\Delta W_s = 8\pi K_s \Delta r^2 \quad (3)$$

Meanwhile, the work done by the electroosmotic force during the elongation half cycle of the membrane inside the micropipet can be expressed as

$$W_{eo} = \int_l^{l+\Delta l} F_{eo}(t) dl \propto \int_l^{l+\Delta l} V(t) dl \propto \int_0^{1/2f} V_0 \sin(2\pi ft) dt = \frac{V_0}{\pi f} \quad (4)$$

where l and $l + \Delta l$ represent the original and final lengths of the vesicle protrusion inside the micropipet, V_0 is the amplitude of driving voltage, and f is the driving frequency. Here, we assume that the velocity of the electroosmotic flow remains constant during the elongation period. From energy conservation, $\Delta W_s = W_{eo}$, and therefore we have $\Delta r^2 \propto V_0/\pi f$, or the measured deformation is in proportion to $1/\sqrt{f}$. This energy-conservation model is in agreement with the data in Figure 6. The above analyses can help us understand the characteristics of the electrically driven vesicle deformation on the basis of the electroosmotic effect of the micropipet.

Voltage-Induced Deformation of DPPC:Cholesterol Vesicles. In the electroosmotic modeling of the voltage-induced vesicle deformation, a key parameter of the membrane is the area compressibility K_s . Therefore, the characteristics of the electrically driven deformation must be different for vesicles made of a membrane with a different K_s . It is known that cholesterol increases the area compressibility of lipid membranes.^{5,16,17} We used DPPC:cholesterol vesicles as a further test to the above model. The cholesterol was also from Sigma-Aldrich. We blended the powders of DPPC and cholesterol and then

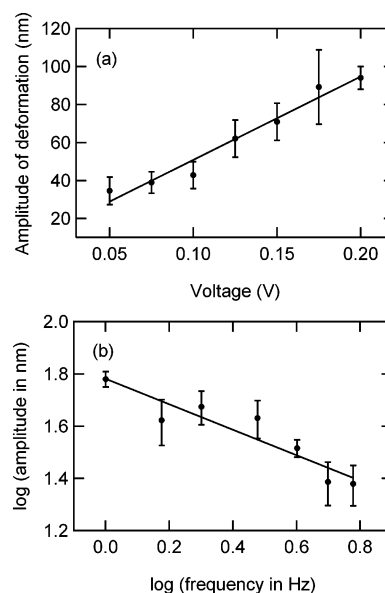


Figure 8. (a) Deformation of a DPPC:cholesterol vesicle driven at 3 Hz. Dots, membrane amplitudes. The error bars represent the standard deviation of three measurements. Solid line, a linear fitting shows that the deformation is still proportional to the driving voltage. (b) Frequency response of the deformation driven at 0.1 V. Solid line, a fitting line of which the slope is -0.49 ± 0.09 . During the measurement, the temperature was kept at 23 °C.

prepared the vesicles following the same procedures described in the Materials and Methods section. The molar fraction of cholesterol was 0.65.

Figure 8a shows the voltage response of a 14- μ m DPPC:cholesterol vesicle. The linear response is similar to that of a pure DPPC vesicle shown in Figure 5, but the deformations are much smaller. Because the area compressibility was increased by cholesterol, a same change in surface area corresponded to larger tension according to eq 1. Therefore, at a given driving voltage, the electroosmotic force must be balanced at a smaller deformation of the vesicle. The frequency response of the same DPPC:cholesterol vesicle is shown in Figure 8b. We found that the slope is -0.49 ± 0.09 , which again agrees with the above energy-conservation model. However, the present qualitative modeling is not sufficient for us to deduce the area compressibility from the deformation.

Voltage-Induced Membrane Motion in the Fluid Phase. The mechanical properties of GLV membranes are dissimilar in different phases. For example, the bending rigidity decreases by an order of magnitude from the gel phase to the fluid phase.^{9,18} Therefore, the electrically driven deformations in the fluid phase could be very different from that in the gel phase. The main transition temperature of DPPC membranes has been determined to be 41.5 °C.¹⁹ As we increased the temperature to 47 °C, the voltage-induced membrane motion is shown in Figure 9a, and the corresponding spectrum is shown in Figure 9b. The spectrum in Figure 9b shows that the membrane motion does not correlate to the driving signal. The submicrometer deformation seems to be overwhelmed by the micrometer-scale thermal fluctuations of the fluid membrane.

Discussion. The optical measurement in this study has the following features. (1) Without mechanical contact,

(15) Petrov, A. G. *The Lyotropic State of Matter: Molecular Physics and Living Matter Physics*; Gordon and Breach Science Publishers: Amsterdam, 1999; Chapter 4.

(16) Needham, D.; McIntosh, T. J.; Evans, E. *Biochemistry* **1988**, *27*, 4668–4673.

(17) Needham, D.; Nunn, R. S. *Biophys. J.* **1990**, *58*, 997–1009.

(18) Mecke, K. R.; Charitat, T.; Graner, F. *Langmuir* **2003**, *19*, 2080–2087.

(19) Heimburg, T. *Biochim. Biophys. Acta* **1998**, *1415*, 147–162.

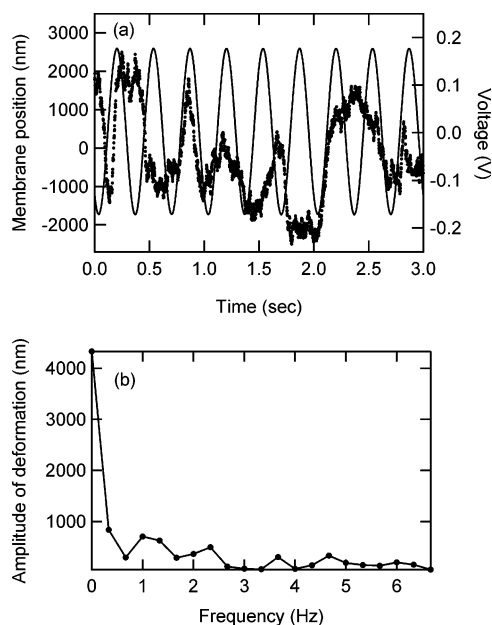


Figure 9. (a) Deformation of a 40- μm DPPC vesicle in the fluid phase caused by 0.17 V driving voltage. Dots, membrane position. Solid line, applied voltage. The modulation frequency is 3 Hz. (b) Spectrum of the membrane movements in a. During the measurement, the temperature was kept at 47 $^{\circ}\text{C}$.

we can study a single GLV under various modulating and environmental conditions. The vesicle stayed intact throughout the measurement, and therefore the comparisons at various modulating or environmental conditions are simple. (2) On the basis of the large deformation, it is possible to employ GLVs as electrically driven mechanical actuators in microfluidic systems. The micropipet can also be used to hold and place the vesicle to a specific site. (3) For gel-phase GLVs of different

components, the data are in agreement with a simple model on the basis of the electroosmotic effect of the micropipet. However, at present, we only qualitatively explain the features of the electrically driven deformation. Quantitative analysis of this phenomenon requires more complicated modeling and numerical simulations of the electroosmotic flow of a cell-attached clamp scheme.

Conclusions

Optical measurement of the electrically driven deformation of GLVs was performed by using differential confocal microscopy. A voltage-clamped vesicle in the cell-attached configuration could be studied under various driving signals and in different phases without the risk of membrane perforation. Deformations as large as hundreds of nanometers were measured when a 0.1 V square wave was applied on a DPPC vesicle. In the low-temperature gel phase, we found a linear relation between the deformation and the driving voltage, which can be explained by the electroosmotic effect in the micropipet. The electrically driven deformation is proportional to the square root of the inverse of the driving frequency. This characteristic can be explained by the energy conservation between the electroosmotic force and the membrane stretching elasticity. We also used DPPC:cholesterol vesicles to test this model and obtained consistent results. Because the only parameter of membrane in this model is the area compressibility, we believe that similar results can be found on GLVs made of other materials, such as polymers.^{20,21} GLVs with such electrically driven deformations may be used as actuators in microfluidic systems. In the fluid phase, electrically driven movements were not observed because thermal fluctuations dominated the membrane motion.

LA051248A

(20) Helfer, E.; Harlepp, S.; Bourdieu, L.; Robert, J.; MacKintosh, F. C.; Chatenay, D. *Phys. Rev. Lett.* **2000**, *85*, 457–460.

(21) Discher, D. E.; Eisenberg, A. *Science* **2002**, *297*, 967–973.